A Generalized Multiscale Finite Element Method for Thermoelasticity Problems

Maria Vasilyeva[1,2(✉)] and Denis Stalnov[1]

[1] North-Eastern Federal University, Yakutsk, Russia
vasilyevadotmdotv@gmail.com
[2] Texas A&M University, College Station, TX, USA

Abstract. In this work, we consider the coupled systems of a partial differential equations, which arise in the modeling of thermoelasticity processes in heterogeneous domains. Heterogeneity of the properties requires a high resolution solve that adds many degrees of freedom that can be computationally costly. For the numerical solution, we use a Generalized Multiscale Finite Element Method (GMsFEM) that solves problem on a coarse grid by constructing local multiscale basis functions [1–3]. We construct multiscale basis functions for the temperature and for the displacements on the offline stage in each coarse block using local spectral problems [4–7]. On the online stage we construct coarse scale system using precalculated multiscale basis functions and solve problem with any forcing and boundary conditions. The numerical results are presented for heterogeneous and perforated domains.

1 Problem Formulation and Fine Scale Approximation

We consider linear thermoelasticity problem for temperature, T, and for displacement, u [8–10]

$$\begin{aligned} -\operatorname{div}\sigma(u) + \beta \operatorname{grad} T &= 0 \text{ in } \Omega, \\ \beta \operatorname{div}\frac{\partial u}{\partial t} + c\frac{\partial T}{\partial t} - \operatorname{div}(k \operatorname{grad} T) &= f \text{ in } \Omega, \end{aligned} \tag{1}$$

where f is a source term, c is a heat capacity, k is a thermal conductivity and β is the coupling coefficient.

The stress and strain tensors are given by

$$\sigma(u) = 2\mu\varepsilon(u) + \lambda \operatorname{div}(u)\mathcal{I}, \quad \varepsilon(u) = \frac{1}{2}\left(\operatorname{grad} u + \operatorname{grad} u^T\right),$$

where μ, λ are Lame parameters, $\mathcal{I}$ is the identity tensor.

We consider (1) with initial condition $T(x,0) = T_0$ and boundary conditions for displacement and for temperature

$$\sigma n = 0, \quad x \in \Gamma_N^u, \quad u = u_1, \quad x \in \Gamma_D^u,$$

I. Dimov et al. (Eds.): NAA 2016, LNCS 10187, pp. 713–720, 2017.
DOI: 10.1007/978-3-319-57099-0_82

$$-k\frac{\partial T}{\partial n} = 0, \quad x \in \Gamma_N^T, \quad T = T_1, \quad x \in \Gamma_D^T,$$

where n is the unit normal to the boundary.

For numerical solution on fine grid, we use a standard finite element method and implicit scheme for approximation by time [4,5,8]

$$\begin{aligned} a_u(u^{n+1}, v) + b(T^{n+1}, v) &= 0, \\ b(u^{n+1} - u^n, q) + m(T^{n+1} - T^n, q) + \tau a_T(T^{n+1}, q) &= \tau(f, q), \end{aligned} \tag{2}$$

for $(u, T) \in W = (V, Q)$ and $(v, q) \in \hat{W} = (\hat{V}, \hat{Q})$ where

$$\begin{aligned} V &= \{v \in [H^1(\Omega)]^d : v(x) = u_1, x \in \Gamma_D^u\}, \quad Q = \{q \in H^1(\Omega) : q(x) = T_1, x \in \Gamma_D^T\}, \\ \hat{V} &= \{v \in [H^1(\Omega)]^d : v(x) = 0, x \in \Gamma_D^u\}, \quad \hat{Q} = \{q \in H^1(\Omega) : q(x) = 0, x \in \Gamma_D^T\}. \end{aligned}$$

Here for bilinear and linear forms we have

$$\begin{aligned} a_u(u, v) &= \int_\Omega (\sigma(u), \varepsilon(v)) dx, \quad a_T(T, q) = \int_\Omega (k \operatorname{grad} T, \operatorname{grad} q)\, dx, \\ b(T, u) &= \int_\Omega \beta(\operatorname{grad} T, u) dx, \quad m(T, q) = \int_\Omega c\, T\, q\, dx, \quad (f, q) = \int_\Omega f\, q\, dx. \end{aligned}$$

where as basis functions on fine grid we use standard linear basis functions for both temperature and displacement.

2 Coarse-Scale Approximaiton Using GMsFEM

Let $\mathcal{T}^H$ be a standard conforming partition of the computational domain Ω into finite elements. We refer to this partition as the coarse-grid and assume that each coarse element is partitioned into a connected union of fine grid blocks. The fine grid partition will be denoted by $\mathcal{T}^h$. Let $\{x_i\}_{i=1}^N$ is the vertices of the coarse mesh $\mathcal{T}^H$, where N is the number of coarse nodes. We define the neighborhood (local) domain of the node x_i by

$$\omega_i = \bigcup_j \left\{ K_j \in \mathcal{T}^H \,|\, x_i \in \overline{K}_j \right\},$$

where K_j to denote a coarse element.

In the GMsFEM algorithm, we have three steps [1–3]:

Step 1: Generate the coarse-grid, $\mathcal{T}^H$ and local domains ω_i, $i = 1, 2, \ldots, N$;
Step 2: The construction of the multiscale basis functions in local domains, ω_i, $i = 1, 2, \ldots, N$ (offline space);
Step 3: Use offline space to find the solution of a coarse-grid problem for any force term and/or boundary conditions.

We construct multiscale basis functions for temperature and displacements separately.

Multiscale Basis Functions for Pressure. To construct the offline space Q_{off} for temperature, we solve following the eigenvalue problem in the local domain ω:

$$A_T \Psi_k^{\text{off}} = \lambda_k^{\text{off}} S_T \Psi_k^{\text{off}},$$
$$A_T = [a_{ij}], \quad a_{ij} = \int_\Omega (k \operatorname{grad} \phi_i, \operatorname{grad} \phi_j)\, dx, \quad M_T = [s_{ij}], \quad s_{ij} = \int_\Omega k \phi_i \phi_j\, dx, \tag{3}$$

and choose the eigenvectors ψ_k^{off} that corresponds to the smallest $M_{\text{off}}^{\omega,T}$ eigenvalues in Eq. (3) and denote the span of this reduced space as Q_{off}^{ω}.

For construction of the offline space, to ensure the functions we construct form an conforming basis, we define multiscale partition of unity functions χ_i

$$a_T(\chi_i, q) = 0 \quad \text{in } K, \quad \chi_i = g_i \quad \text{on } \partial K, \tag{4}$$

for all $K \in \omega$. Here g_i is a continuous on K and is linear on each edge of ∂K.

Finally, we multiply the partition of unity functions by the eigenfunctions in the offline space $Q_{\text{off}}^{\omega_i}$ to construct the resulting basis functions $\psi_{i,k} = \chi_i \psi_k^{\omega,\text{off}}$, for $1 \le i \le N$ and $\le k \le M_{\text{off}}^{\omega_i,T}$, where $M_{\text{off}}^{\omega_i,T}$ denotes the number of offline eigenvectors that are chosen for each coarse node i.

We define the multiscale space using a single index notation as

$$Q_{\text{off}} = \operatorname{span}\{\psi_i\}_{i=1}^{M_T^{\text{off}}}, \quad \text{and} \quad R_T = \left[\psi_1, \ldots, \psi_{M_T^{\text{off}}}\right]^T, \tag{5}$$

where $M_T^{\text{off}} = \sum_{i=1}^{N} M_{\text{off}}^{\omega_i,T}$ denotes the total number of basis functions.

Multiscale Basis Functions for Displacement. For construction of multiscale basis functions for displacements we use similar algorithm that we used for the temperature. We solve the following eigenvalue problem in $V_h(\omega)$ [3–5]

$$A_u \Phi_k^{\text{off}} = \lambda_k^{\text{off}} S_u \Phi_k^{\text{off}},$$
$$A_u = [a_{ij}], \quad a_{ij} = \int_\Omega \Big(2\mu\varepsilon(\varphi_m) : \varepsilon(\varphi_n) + \lambda \operatorname{div}(\varphi_m) \cdot \operatorname{div}(\varphi_n)\Big), \tag{6}$$
$$S_u = [s_{ij}], \quad s_{ij} = \textstyle\int_\Omega (\lambda + 2\mu)\varphi_m \cdot \varphi_n.$$

We then choose the eigenvectors that corresponds to the smallest $M_{\text{off}}^{\omega,u}$ eigenvalues from Eq. (6) and denote the span of this reduced space as V_{off}^{ω}.

For construction of multiscale partition of unity functions for the mechanics solve, we proceed as before and solve for all $K \in \omega$

$$a_u(\xi_i, v) = 0 \quad \text{in } K, \quad \xi_i = g_i \quad \text{on } \partial K, \tag{7}$$

where g_i is a continuous function on K and is linear on each edge of ∂K. Finally, we multiply the partition of unity functions by the eigenfunctions in the offline space $V_{\text{off}}^{\omega_i}$ to construct the resulting basis functions $\varphi_{i,k} = \xi_i \varphi_k^{\omega_i,\text{off}}$ for $1 \le i \le N$ and $1 \le k \le M_{\text{off}}^{\omega_i,u}$, where $M_{\text{off}}^{\omega_i,u}$ denotes the number of offline eigenvectors that are chosen for each coarse node i.

Next, we define the multiscale space as

$$V_{\text{off}} = \text{span}\{\varphi_i\}_{i=1}^{M_u^{\text{off}}}, \quad \text{and} \quad R_u = \left[\psi_1, \ldots, \varphi_{M_u^{\text{off}}}\right]^T, \tag{8}$$

where $M_u^{\text{off}} = \sum_{i=1}^{N} M_{\text{off}}^{\omega_i, u}$ denotes the total number of basis functions.

Coarse-Scale System. The variational form in (2) yields the following linear algebraic system

$$\begin{pmatrix} A_u^c & (B_c)^T \\ B^c & (M_c + \tau A_T^c) \end{pmatrix} \begin{pmatrix} u_H^{n+1} \\ T_H^{n+1} \end{pmatrix} = \begin{pmatrix} 0 \\ Q_c \end{pmatrix}, \tag{9}$$

where

$$A_u^c = R_u A_u R_u^T, \quad A_T^c = R_T A_T R_T^T \quad B_c = R_T B R_u^T, \quad M_c = R_T M R_T^T$$

and $Q_c = R_T \tau F + M_c T_H^n + B_c u_H^n$. Here u_H and T_H denotes the coarse-scale solutions that we can project into the fine-grid $u_h^{n+1} = R_u^T u_H^{n+1}$ and $T_h^{n+1} = R_T^T T_H^{n+1}$.

3 Numerical Examples

In this section, we present numerical examples to demonstrate the performance of the GMsFEM for computing the solution of the thermoelasticity problem in heterogeneous and perforated domains where the inclusions can have different size (see Figs. 1 and 2).

We present results for perforated and heterogeneous domains with random distribution of the inclusions (Fig. 1). For high-constrast domain, we consider case with one type of particles (Fig. 2). For numerical simulations we use following thermomechanical coefficients: $c_1 = 1000$, $c_2 = 100$, $k_1 = 1$, $k_2 = 100$, $E_1 = 100$, $E_2 = 10$, $\nu = 0.3$ and $\beta = 1.0$.

We consider three test cases:

Case 1a. Perforated domain with homogeneous backround with source term $f = 100$ and zero Dirichlet boundary conditions for temperature and displacement on perforations;
Case 1b. Perforated domain with heterogeneous backround with source term $f = 100$ and zero Dirichlet boundary conditions for temperature and displacement on perforations;
Case 2. Heterogeneous domain with circle particles with zero source term $f = 0$ and boundary conditions: a fixed temperature $T = 1.0$ on cavity, a fixed displacements $u_x = 0$ for left boundary and $u_y = 0$ on top boundary.

For numerical comparison, we calculate a weighted relative errors using L^2 norm and H^1 semi-norm for temperature

$$||\epsilon_T||_{L^2} = \left(\int_\Omega k \epsilon_T^2 dx \right)^{1/2}, \quad |\epsilon_T|_{H^1} = \left(\int_\Omega (k \,\text{grad}\, \epsilon_T, \text{grad}\, \epsilon_T)\, dx \right)^{1/2},$$

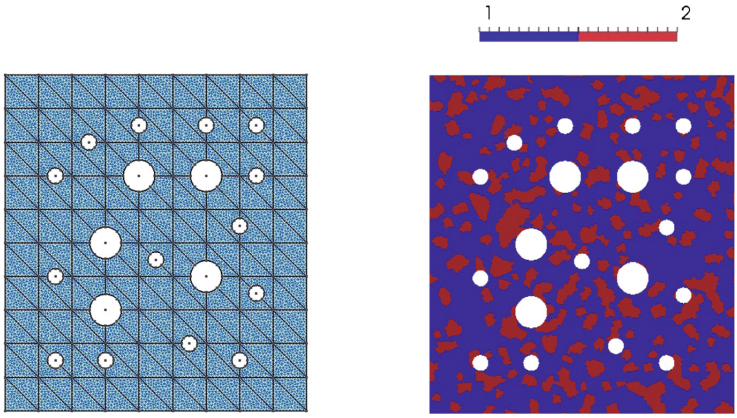

Fig. 1. Coarse and fine computational grids (left) and heterogeneous backround (right). Blue color is the subdomain 2 and red is the subdomain 1. Fine grid contains 12426 vertices and 24124 cells. Coarse grid have 110 vertices and 180 cells. (Color figure online)

and for displacement

$$||\epsilon_u||_{L^2} = \left(\int_\Omega (\lambda + 2\mu)(\epsilon_u, \epsilon_u) dx \right)^{1/2}, \quad |\epsilon_u|_{H^1} = \left(\int_\Omega (\sigma(\epsilon_u), \varepsilon(\epsilon_u))\, dx \right)^{1/2},$$

where $\epsilon_T = T_f - T_{ms}$, $\epsilon_u = u_f - u_{ms}$. Here (u_f, T_f) and (u_{ms}, T_{ms}) are fine-scale and coarse-scale (multiscale) solutions, respectively for displacement and temperature.

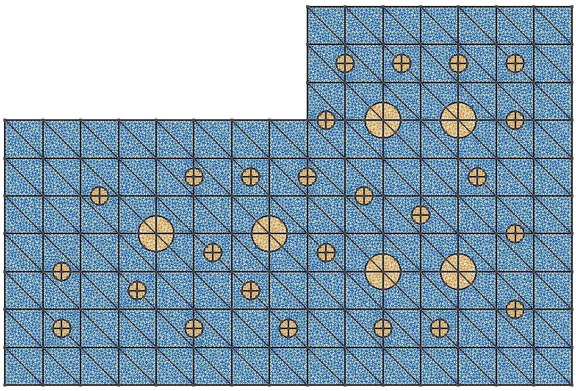

Fig. 2. Coarse and fine computational grids (left) for domain with circle particles. Orange color is the subdomain 2 and blue is the subdomain 1. Fine grid contains 18378 vertices and 36254 cells. Coarse grid have 152 vertices and 252 cells. (Color figure online)

Table 1. Relative L_2 and H_1 errors for temperature and displacement in percentage

$M_T^{off} = M_u^{off}$	$dim(W^{off})$	Temperature errors, ϵ^T		Displacement errors, ϵ^u	
		$\epsilon^T_{L^2}$	$\epsilon^T_{H^1}$	$\epsilon^u_{L^2}$	$\epsilon^u_{H_1}$
Perforated domain, *Case 1a*					
2	660	7.08	27.07	18.55	45.05
4	1320	2.48	15.22	6.63	27.32
8	2640	0.72	7.60	1.94	14.53
16	5280	0.20	3.65	0.43	6.01
Perforated domain with heterogeneous backround, *Case 1b*					
2	660	47.03	71.60	61.57	70.29
4	1320	17.74	45.50	26.16	43.28
8	2640	1.42	16.73	5.07	22.19
16	5280	0.20	6.37	0.98	10.14
20	6600	0.13	4.76	0.61	7.83
Heterogeneous domain with circle particles, *Case 2*					
2	912	6.085	43.48	11.33	32.25
4	1824	4.81	19.05	7.17	25.76
8	3648	3.06	12.55	1.23	14.86
16	7296	1.47	7.41	0.43	9.05
20	9120	1.15	6.53	0.82	7.53

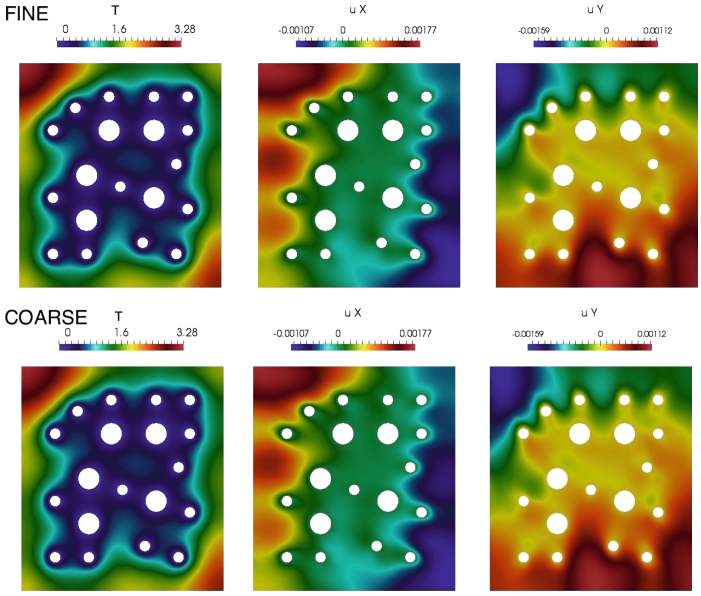

Fig. 3. Fine-scale solution (top) and coarse-scale solution using 8 basis functions for temperature and 8 for displacement (bottom) for the *Case 1a*. Left: temperature. Middle: displacement u_x. Right: displacement u_y.

In Fig. 3, we show the fine-scale and coarse-scale solutions for the *Case 1a* and in Fig. 4 for the *Case 1b*. For multiscale solution we used 8 multiscale basis functions for temperature and 8 multiscale basis functions for displacement. Comparing the fine-scale and coarse-scale solutions in Figs. 3 and 4, we can

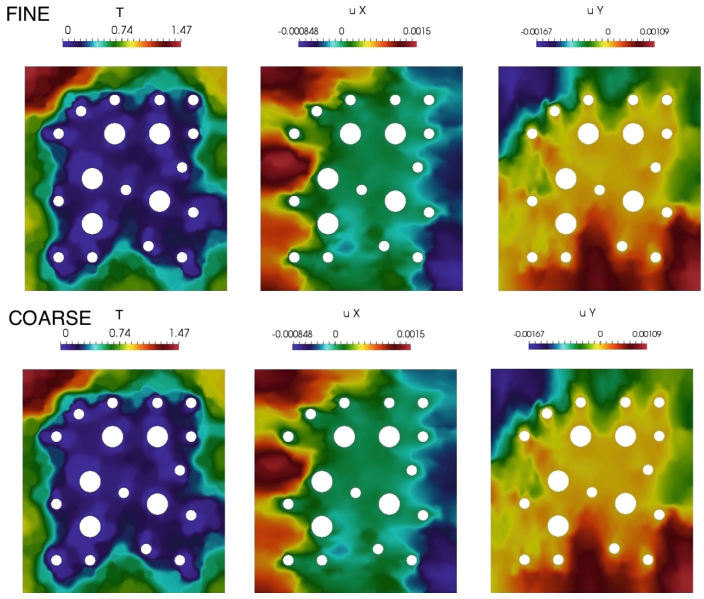

Fig. 4. Fine-scale solution (top) and coarse-scale solution using 8 basis functions for temperature and 8 for displacement (bottom) for the *Case 1b*. Left: temperature. Middle: displacement u_x. Right: displacement u_y.

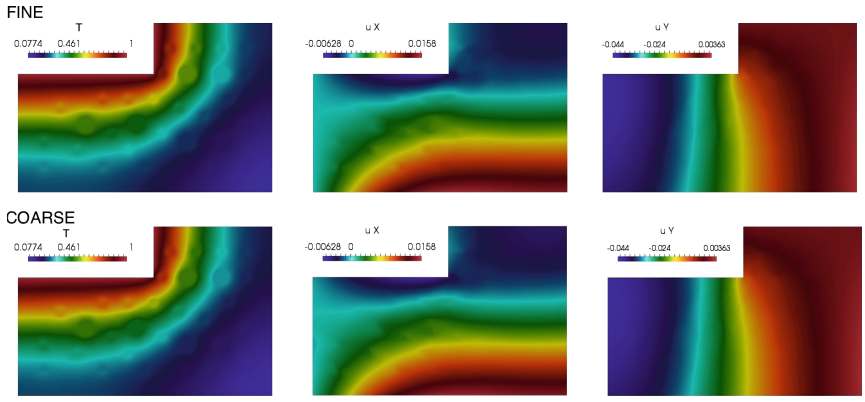

Fig. 5. Fine-scale solution (top) and coarse-scale solution using 8 basis functions for temperature and 8 for displacement (bottom) for the *Case 2*. Left: temperature. Middle: displacement u_x. Right: displacement u_y.

observe a good accuracy of the proposed multiscale method for both homogeneous and heterogeneous backround coefficients for perforated domain. In Fig. 5 we show solutions for the *Case 2* for heterogeneous domain with circle particles. In Table 1 we present relative errors for the coarse-scale solutions with different number of the multiscale basis functions. We observe a good accuracy for all cases for multiscale solution using only $\approx 0.2\%$ of fine-scale system size.

Acknowledgement. We would like to thank Professor Yalchin Efendiev for many interesting discussions. This work is partially supported by the grant of the President of the Russian Federation MK-9613.2016.1 and RFBR (project N 15-31-20856).

References

1. Efendiev, Y., Galvis, J., Hou, T.: Generalized multiscale finite element methods. J. Comput. Phys. **251**, 116–135 (2013)
2. Efendiev, Y., Hou, T.: Multiscale Finite Element Methods: Theory and Applications. Surveys and Tutorials in the Applied Mathematical Sciences, vol. 4. Springer, New York (2009)
3. Chung, E.T., Efendiev, Y., Li, G., Vasilyeva, M.: Generalized multiscale finite element method for problems in perforated heterogeneous domains. Appl. Anal. **255**, 1–15 (2015)
4. Brown, D.L., Vasilyeva, M.: A generalized multiscale finite element method for poroelasticity problems I: linear problems. J. Comput. Appl. Math. **294**, 372–388 (2016)
5. Brown, D.L., Vasilyeva, M.: A generalized multiscale finite element method for poroelasticity problems II: nonlinear coupling. J. Comput. Appl. Math. **297**, 132–146 (2016)
6. Chung, E.T., Efendiev, Y., Leung, W.T., Vasilyeva, M., Wang, Y.: Online adaptive local multiscale model reduction for heterogeneous problems in perforated domains (2016). arXiv preprint arXiv:1605.07645
7. Chung, E.T., Efendiev, Y., Gibson, R., Vasilyeva, M.: A generalized multiscale finite element method for elastic wave propagation in fractured media. GEM-Int. J. Geomath. 1–20 (2015)
8. Kolesov, A.E., Vabishchevich, P.N., Vasilyeva, M.V.: Splitting schemes for poroelasticity and thermoelasticity problems. Comput. Math. Appl. **67**(12), 2185–2198 (2014)
9. Mikelic, A., Wheeler, M.F.: Convergence of iterative coupling for coupled flow and geomechanics. Comput. Geosci. **17**, 1–7 (2013). Springer
10. Kim, J., Tchelepi, H.A., Juanes, R.: Stability, accuracy, and efficiency of sequential methods for coupled flow and geomechanics. SPE J. **16**(2), 249–262 (2011)